

Reactions of Pyridyl-Functionalized, Chelating λ^3 -Phosphanes in the Coordination Environment of Rh^{III} and Ir^{III}

Iris de Krom,^[a] Evgeny A. Pidko,^[a] Martin Lutz,^[b] and Christian Müller*^[a, c]

Dedicated to Professor Werner Uhl on the occasion of his 60th birthday

Abstract: Rh^{III} and Ir^{III} complexes based on the λ^3 -P,N hybrid ligand 2-(2'-pyridyl)-4,6-diphenylphosphinine (**1**) react selectively at the P=C double bond to chiral coordination compounds of the type $[(1\text{H}\cdot\text{OH})\text{Cp}^*\text{MCl}]\text{Cl}$ (**2,3**), which can be deprotonated with triethylamine to eliminate HCl. By using different bases, the $\text{p}K_{\text{a}}$ value of the P–OH group could be estimated. Whereas $[(1\text{H}\cdot\text{O})\text{Cp}^*\text{IrCl}]$ (**4**) is formed quan-

titatively upon treatment with NEt_3 , the corresponding rhodium compound $[(1\text{H}\cdot\text{O})\text{Cp}^*\text{RhCl}]$ (**5**) undergoes tautomerization upon formation of the $\lambda^5\sigma^4$ -phosphinine rhodium(III) complex $[(1\cdot\text{OH})\text{Cp}^*\text{RhCl}]$ (**6**) as confirmed by

Keywords: chelates • coordination chemistry • heterocycles • N,P ligands • phosphorus

single-crystal X-ray diffraction. Blocking the acidic P–OH functionality in **3** by introducing a P–OCH₃ substituent leads directly to the $\lambda^5\sigma^4$ -phosphinine iridium(III) complex (**8**) upon elimination of HCl. These new transformations in the coordination environment of Rh^{III} and Ir^{III} provide an easy and general access to new transition-metal complexes containing $\lambda^5\sigma^4$ -phosphinine ligands.

Introduction

2,2'-Bipyridine derivatives are well-studied bidentate nitrogen ligands and their corresponding transition-metal complexes find widespread application in various areas of chemistry, such as molecular electronics, homogeneous catalysis, or material science.^[1] The replacement of a pyridine unit by a π -accepting λ^3 -phosphinine entity^[2,3] leads to 2-(2'-pyridyl)phosphinine, a semi-equivalent of 2,2'-bipyridine. Such chelates are intriguing ligands that contain a low-coordinate “soft” phosphorus and a “hard” nitrogen heteroatom. The first example of this type of P,N hybrid ligand has been described by Mathey et al. in 1982 with the synthesis of 2-(2'-pyridyl)-4,5-dimethylphosphinine (NIPHOS, Figure 1).^[4] We have recently developed a facile synthetic route to 2-(2'-pyridyl)-4,6-diphenylphosphinine (**1**, Figure 1), which is readily

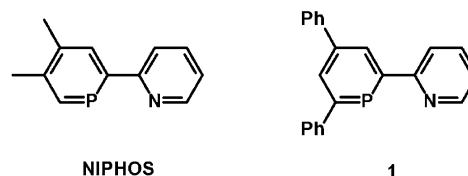


Figure 1. Pyridyl-functionalized phosphinines NIPHOS and 2-(2'-pyridyl)-4,6-diphenylphosphinine **1**.

available from the corresponding pyridyl-functionalized pyrylium salt.^[5–7]

It is by now well established that the coordination chemistry of phosphorus-analogues of 2,2'-bipyridines is markedly different from that of classical tertiary diphosphines or their all-nitrogen-counterparts.^[8–12] In contrast to (bi)pyridines, phosphinine-based ligands are especially suitable for the stabilization of electron-rich metal centers due to the pronounced π -acceptor properties of the aromatic phosphorus heterocycle.^[8–13]

On the other hand, the aromaticity of the phosphinine heterocycle is significantly disrupted upon coordination to metal centers in especially higher oxidation states and with reduced π -back-donation capability. Accordingly, the phosphinine core behaves like a cyclophosphahexatriene containing a highly reactive P=C double bond.^[14] Venanzi et al. have shown that cationic Pd^{II} and Pt^{II} complexes of NIPHOS react with traces of water and alcohols to the corresponding dihydrophosphinine species of type **A** (Figure 2).^[15] The regioselective addition of methanol exclusively to the external P=C_α double bond can be attributed to the somewhat higher nucleophilicity of the external C_α-atom due to the electron-withdrawing character of the pyridine ring connected to the internal C_α atom, leading to a prefer-

[a] I. de Krom, Dr. E. A. Pidko, Prof. Dr. C. Müller
Chemical Engineering and Chemistry
Eindhoven University of Technology
Den Dolech 2, 5600 MB Eindhoven (The Netherlands)

[b] Dr. M. Lutz
Bijvoet Center for Biomolecular Research
Utrecht University
Padualaan 8, 3584 CH Utrecht (The Netherlands)

[c] Prof. Dr. C. Müller
Institut für Chemie und Biochemie
Anorganische Chemie
Freie Universität Berlin
Fabeckstrasse 34–36, 14195 Berlin (Germany)
Fax: (+49) 30-83852440
E-mail: c.mueller@fu-berlin.de

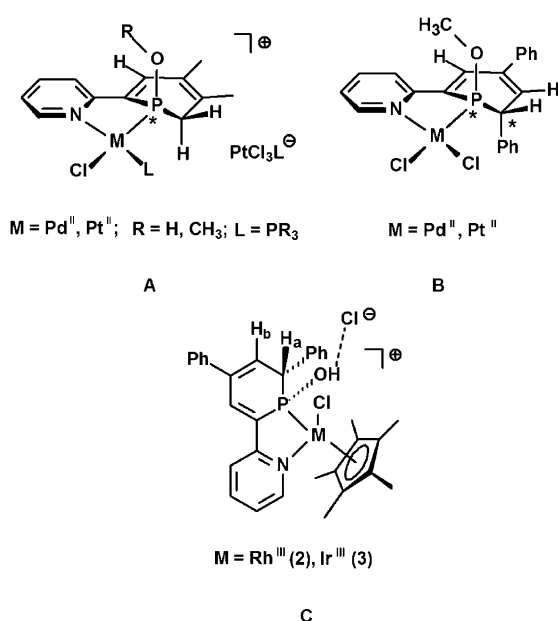


Figure 2. Coordination compounds **A–C** containing dihydrophosphinine ligands.

red addition of the proton exclusively to the external C_α-atom.^[7] Nevertheless, as the external C_α-atom in NIPHOS is not prochiral, the structural characterization of **A** does not allow one to draw any conclusion as to whether the addition of ROH to the P=C double bond proceeds in a *syn*- or *anti*-fashion, or even randomly.

Interestingly, the pyridyl-functionalized phosphinine **1** does contain a prochiral center at the external C_α-atom, providing the possibility to gain more insight into the mechanism of the addition process once the ligand is coordinated to a metal center. As a matter of fact, we could recently demonstrate for the first time that the reaction of the neutral phosphinine-M^{II} complexes [(**1**)PdCl₂] and [(**1**)PtCl₂] with MeOH does not proceed randomly but quantitatively and selectively to the *syn*-addition product of type **B** (Figure 2) as confirmed by the X-ray crystal structure.^[7] This indicates that the reaction proceeds in a concerted way, rather than in a two-step process. In contrast, we found that treatment of the cationic phosphinine-M^{III} complexes [(**1**)Cp*RhCl]Cl and [(**1**)Cp*IrCl]Cl with water leads quantitatively and selectively to the *anti*-addition products **2** (Rh) and **3** (Ir), respectively (type **C**, Figure 2), as confirmed by crystal structure determinations.^[16] Additionally, hydrogen bonding between the –OH hydrogen atom and the Cl[–] counteranion was observed.

Venanzi et al. have already demonstrated that the –OH group in [(NIPHOSH–OH)(L)PtCl]⁺ (**A**, Figure 1) can be deprotonated with diisopropylamine to form [(NIPHOSH–O)PtCl(L)], al-

though the product was never structurally characterized.^[15] We have now started to investigate the reaction of racemic mixtures of chiral phosphinine-metal complexes with water and alcohols in more detail and report here on reactions of the P,N hybrid ligand **1** in the coordination environment of Rh^{III} and Ir^{III}.

Results and Discussion

Figure 3 shows the ¹H NMR spectrum of **3** in CD₂Cl₂ (spectrum 2), which was prepared according to the literature.^[16] The starting material for **3**, [(**1**)Cp*IrCl]Cl, is illustrated as well (spectrum 1) for comparison reasons (see also Scheme 1).^[16]

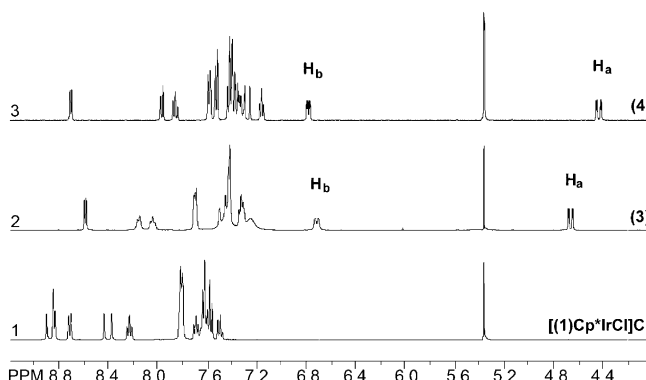
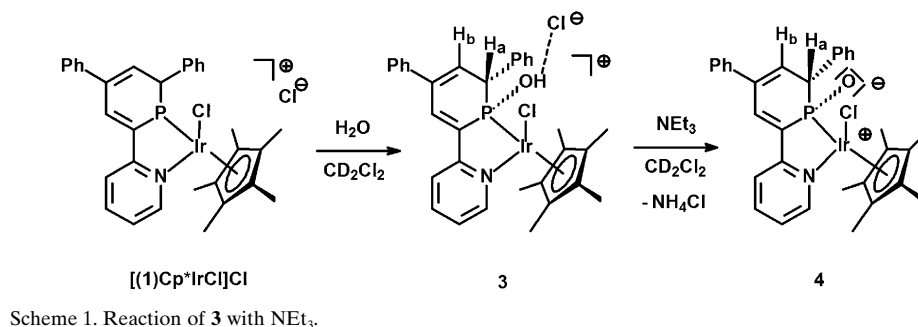


Figure 3. ¹H NMR spectra (CD₂Cl₂) of [(**1**)Cp*IrCl]Cl (bottom), **3** (spectrum 2), and **4** (spectrum 3). The aliphatic region is omitted for clarity.

Compound **3** shows the characteristic resonances for the protons H_a and H_b at δ = 4.61 (dd, ³J_{H–H} = 2.8 Hz; ²J_{H–P} = 12.4 Hz) and 6.66 ppm (d, br, ³J_{H–P} = 9.6 Hz) (see Figure 2, **C**). Upon treating **3** with NEt₃ (≈ 10 equiv) in CD₂Cl₂ the NMR spectroscopic data revealed the clean and quantitative formation of a new species. In the ¹H NMR spectrum (Figure 3, spectrum 3) the signals for the hydrogen atoms H_a and H_b shift from δ = 4.61 to 4.38 ppm (dd, ³J_{H–H} = 3.2 Hz; ²J_{H–P} = 14.0 Hz) and from δ = 6.66 to 6.73 ppm (dd, ³J_{H–H} = 3.2 Hz, ³J_{H–P} = 8.4 Hz). In the ³¹P{¹H} NMR spectrum of the new compound, a shift from δ = 58.0 to 38.9 ppm is observed. On the basis of the NMR spectroscopic data we pro-



Scheme 1. Reaction of **3** with NEt₃.

pose elimination of HCl from [(1H·OH)Cp*IrCl]Cl (**3**) by NEt₃ upon formation of the zwitterionic species **4** according to Scheme 1.

Crystals of **4** suitable for X-ray diffraction were isolated in 54% yield by slow diffusion of Et₂O into a diluted solution of **4** in CD₂Cl₂. The compound crystallizes as a racemate in the orthorhombic space group *Pna*2₁ with one metal complex molecule in the asymmetric unit. The molecular structure is depicted in Figure 4 and selected bonding geometries are compared in Table 1.

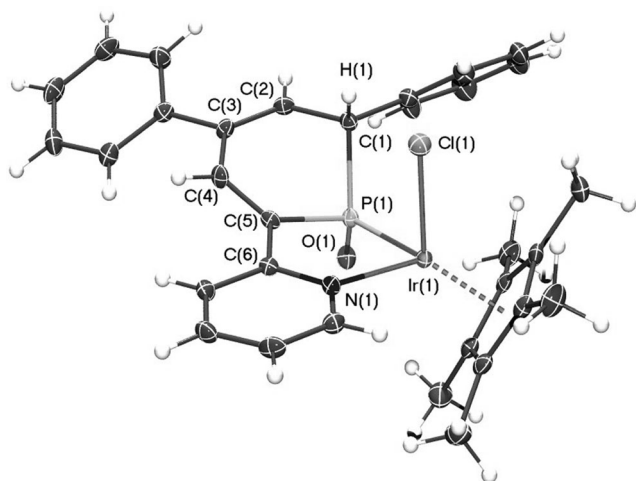


Figure 4. Molecular structure of **4** in the crystal. Displacement ellipsoids are shown at the 50% level.

The molecular structure of **4** in the crystal indeed confirms that elimination of HCl from **3** took place, and the complex can thus best be described as a formally zwitterionic species (Scheme 1). The P(1)–O(1) distance of 1.507(2) Å is somewhat shorter than in **3** (1.5755(18) Å), indicating partial P=O double-bond character. Consequently, the P(1)–C(1) and the P(1)–C(5) distances of 1.863(3) Å and 1.830(3) Å are slightly longer than in **3** (1.827(2) Å and 1.803(2) Å), whereas the C(1)–P(1)–C(5) angle of 95.20(11)° is slightly smaller than in **3** (98.74(11)°). The remaining C–C bond lengths in the phosphorus heterocycle are similar to the ones in **3**.

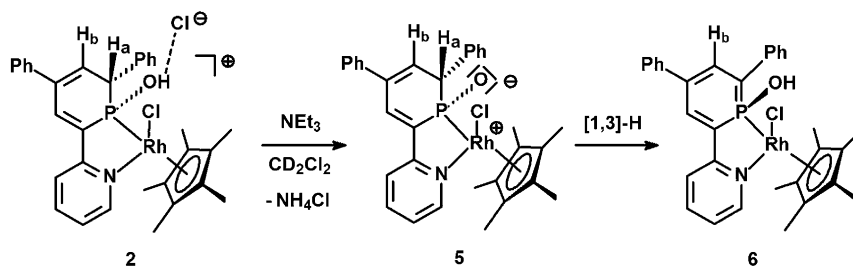
We were further interested in estimating the p*K*_a value of the P–OH functionality in **3**. Whereas addition of NEt₃ (p*K*_b=3.3) to **3** gives quantitative conversion to compound **4** as described above, we added an excess (~10 equiv) of 2,2'-bipyridine (p*K*_b=9.56) to a solution of **3** in CD₂Cl₂. No deprotonation was observed by using ¹H NMR spectroscopy, indicating that the p*K*_a value of the P–OH group is somewhere between p*K*_a=10.7 and 4.35. Addition of pyridine (p*K*_b=

Table 1. Selected bond lengths and angles in compounds **4**, **6**, and **8**.

Compound	4 (Ir)	6 (Rh) (mol. 1)	6 (Rh) (mol. 2)	8 (Ir)
bond lengths [Å]				
M(1) centroid	1.8477(12)	1.8352(12)	1.8324(13)	1.8403(7)
M(1)–Cl(1)	2.4002(7)	2.4075(7)	2.4084(7)	2.4019(4)
P(1)–M(1)	2.2806(7)	2.2791(9)	2.2899(9)	2.2646(4)
N(1)–M(1)	2.115(2)	2.118(2)	2.111(2)	2.1119(13)
P(1)–O(1)	1.507(2)	1.638(2)	1.635(2)	1.6357(11)
P(1)–C(1)	1.863(3)	1.759(3)	1.766(3)	1.7782(15)
P(1)–C(5)	1.830(3)	1.761(3)	1.758(3)	1.7507(16)
C(1)–C(2)	1.510(4)	1.390(4)	1.394(4)	1.371(2)
C(2)–C(3)	1.341(4)	1.411(4)	1.407(4)	1.425(2)
C(3)–C(4)	1.470(4)	1.411(4)	1.394(4)	1.387(2)
C(4)–C(5)	1.336(4)	1.382(4)	1.388(4)	1.404(2)
N(1)–C(6)	1.353(3)	1.366(4)	1.369(4)	1.3724(19)
C(5)–C(6)	1.459(3)	1.448(4)	1.446(4)	1.434(2)
bond angles [°]				
C(1)–P(1)–C(5)	95.20(11)	102.88(13)	103.16(13)	102.52(7)
P(1)–M(1)–N(1)	82.70(6)	76.76(7)	77.41(7)	80.42(4)

8.75), on the other hand, gave a mixture of **3** and **4** in the ratio of 1:2. These results show that the p*K*_a value of the P–OH group is similar to the one of the pyridinium ion, which is p*K*_a=5.25.

Likewise, treatment of **2** (Rh) with NEt₃ (~10 equiv) in CD₂Cl₂ reveals again the predominant formation of a new species. In the ¹H NMR spectrum, the characteristic signals for the hydrogen atoms H_a and H_b shift from δ=4.78 to 4.65 ppm (dd, ³J_{H–H}=3.2 Hz; ²J_{H–P}=12.0 Hz) and from δ=6.53 to 6.63 ppm (dd, ³J_{H–H}=8.0 Hz, ³J_{H–P}=4.0 Hz). In the ³¹P{¹H} NMR spectrum of this compound, a shift from δ=86.0 (d, ¹J_{P–Rh}=133 Hz) to 80.0 ppm (d, ¹J_{P–Rh}=133.0 Hz) is observed. However, after 1 day at room temperature, a minor amount of a second species (~5%) is present in the solution, which shows a single pseudo-triplet at δ=6.80 ppm (³J_{H–P,H–H}=6.0 Hz) in the ¹H NMR spectrum and a doublet (¹J_{P–Rh}=128.8 Hz) at δ=91.0 ppm in the ³¹P{¹H} NMR spectrum. Nevertheless, on the basis of the NMR spectroscopic data we propose again elimination of HCl from [(1H·OH)Cp*RhCl]Cl (**2**) upon formation of the zwitterionic species [(1H·O)Cp*RhCl] (**5**) according to Scheme 2. Crystals suitable for X-ray diffraction were obtained by slow diffusion of diethyl ether into the reaction mixture. The product crystallizes as a racemate in the monoclinic space



Scheme 2. Reaction of **2** with NEt₃.

group *Cc* (No. 9) with two metal-complex molecules in the asymmetric unit. The molecular structure of one enantiomer is depicted in Figure 5 and the selected structure parameters are compared in Table 1. The crystallographic characteriza-

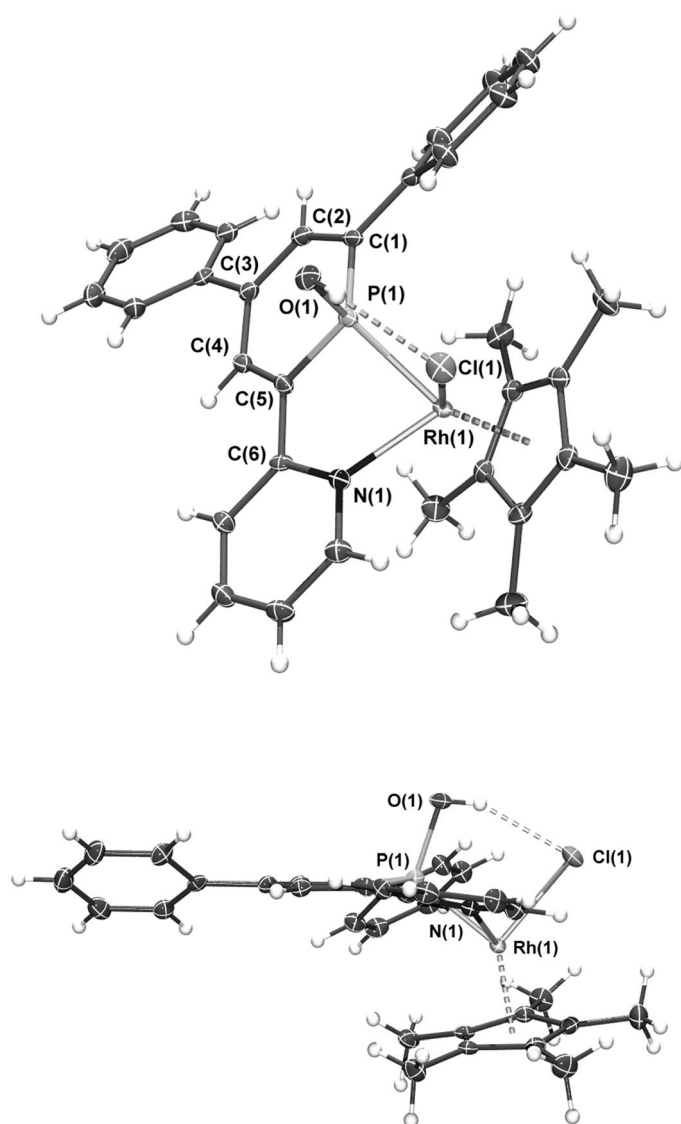


Figure 5. Molecular structure of **6** in the crystal. A noncoordinated CH_2Cl_2 solvent molecule is omitted for clarity. Only one independent molecule is shown. Displacement ellipsoids are shown at the 50% level. Bottom representation: side view.

tion reveals indeed elimination of HCl from **2**. Most strikingly, however, is the fact that the zwitterionic species **5** has not been formed and isolated, but instead its tautomeric form **6**, containing a hydroxyl-group at the phosphorus atom, is present in the solid state (Scheme 2). The minor amount

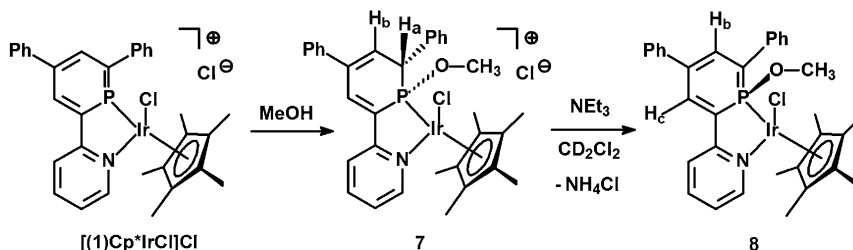
of the second species observed in the ^1H NMR spectrum as mentioned above might thus be attributed to the tautomeric form **6**, which should show a single pseudo-triplet for the proton H_b , due to coupling with the phosphorus nucleus as well as H_c . As a matter of fact, heating a sample of **2** and NEt_3 in CD_2Cl_2 for several hours to $T=60^\circ\text{C}$ reveals that the amount of **6** increases substantially.

The phosphorus heterocycle is essentially planar as observed in the complex $[(1)\text{Cp}^*\text{RhCl}]\text{Cl}$ containing a λ^3 -phosphinine (Figure 5, bottom).

The phosphorus atom escapes from the plane defined by the C1-C2-C3-C4-C5 atoms by only 0.1933(8) Å (Figure 5, bottom view). The P(1)–C(1) and P(1)–C(5) bond lengths in **6** at 1.758(3)–1.766(3) Å are slightly longer than in $[(1)\text{Cp}^*\text{RhCl}]\text{Cl}$ (1.720(2)/1.720(2) Å), whereas the C–C bond lengths in the phosphinine moiety of **6** are essentially identical compared to the ones in $[(1)\text{Cp}^*\text{RhCl}]\text{Cl}$.^[16] The –OH group at the phosphorus atom forms an intramolecular hydrogen-bond to the metal-coordinated chloride. It should be noted here that an inversion of configuration had apparently occurred during the proton-transfer step, either at the phosphorus atom or the Rh center. Both the oxygen atom and the chloride ligand in **6** are now located on the same side of the molecule, which is in contrast to the situation observed in compound **4**.

The deprotonation reactions of **2** and **3** suggest that the $\text{p}K_a$ value of the –OH group is somewhat lower than the one of the $\text{C}_\alpha\text{--H}$ unit, but essentially very similar, as the tautomeric form can apparently be easily formed. We assume that the gain in energy by the more extended delocalization within the phosphorus heterocycle is the driving force for this rearrangement. Taking these results into account, it should be possible to generate the $\lambda^3\sigma^4$ -species directly by deprotonation of a coordination compound, in which no –OH acidic proton is present. We therefore treated $[(1)\text{Cp}^*\text{IrCl}]\text{Cl}$ with an excess of MeOH to form the dihydrophosphinine species **7** (Scheme 3).

Compound **7** shows again the characteristic signals for the hydrogen atoms H_a and H_b at $\delta=4.79$ (dd, $^3J_{\text{H--H}}=3.2$ Hz; $^2J_{\text{H--P}}=11.2$ Hz) and 6.95 ppm (ddd, $^5J_{\text{H--H}}=0.8$ Hz, $^3J_{\text{H--H}}=3.2$ Hz, $^2J_{\text{H--P}}=11.0$ Hz). Moreover, a doublet at $\delta=3.76$ ppm ($^3J_{\text{H--P}}=11.2$ Hz) is observed for the MeO group attached to the phosphorus atom (Figure 6, spectrum 2). In the $^{31}\text{P}\{^1\text{H}\}$ NMR spectrum of **7** a signal at $\delta=77.0$ ppm is observed. Any attempts to grow crystals of compound **7** failed because **7** reacts with traces of water to form coordi-



Scheme 3. Reaction of $[(1)\text{Cp}^*\text{IrCl}]\text{Cl}$ with MeOH and NEt_3 .

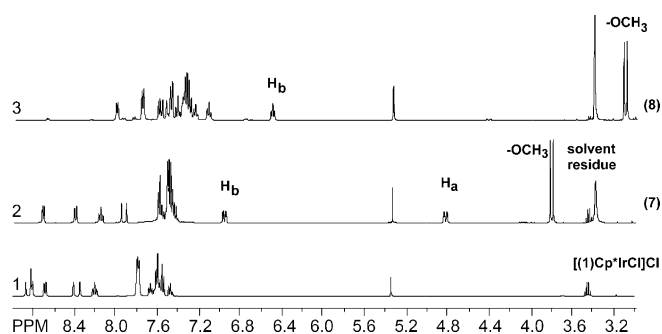
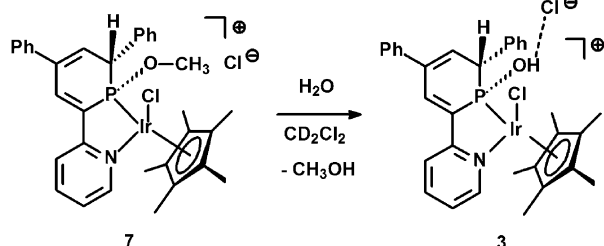


Figure 6. ^1H NMR spectra (CD_2Cl_2) of $[(1)\text{Cp}^*\text{IrCl}]\text{Cl}$ (bottom), **7** (spectrum 2) and **8** (spectrum 3).

nation compound **3**, containing an $-\text{OH}$ functionality rather than an $-\text{OCH}_3$ group at the phosphorus atom (Scheme 4).^[15] We anticipate that the formation of hydrogen bonding between the OH functionality and the Cl counter-anion, as previously observed for **3**, might be the driving force for this process.^[16]



Scheme 4. Reaction of **7** with water under formation of **3**.

Upon treatment of **7** with excess NEt_3 , however, a new species is formed instantaneously, which was apparent from the disappearance of the signal at $\delta = 4.79$ ppm in the ^1H NMR spectrum. Only one pseudo-triplet remains at $\delta = 6.48$ ppm in the ^1H NMR spectrum and one signal at $\delta = 56.0$ ppm observed in the $^{31}\text{P}\{^1\text{H}\}$ NMR spectrum. This result suggests that indeed a deprotonation with the loss of H_a and the formation of a $\lambda^5\sigma^4$ -species (Figure 6, spectrum 3).

Crystals of the new compound were obtained by a slow diffusion of diethyl ether into the reaction mixture. The complex crystallizes as a racemate in the monoclinic space group $P2_1/n$ (No. 14) with one independent molecule in the asymmetric unit. The molecular structure of one enantiomer is depicted in Figure 7 and selected bonding geometries are compared in Table 1. The crystallographic characterization indeed reveals formation of compound **8** according to Scheme 3. The $\text{P}(1)-\text{C}(1)$ and $\text{P}(1)-\text{C}(5)$ bond lengths in **8**, being 1.7782(15) and 1.7507(16) Å, respectively, are longer than in $[(1)\text{Cp}^*\text{IrCl}]\text{Cl}$ (1.717(7)/1.710(6) Å). The C–C bond lengths in the phosphinine moiety of **8** are essentially identical compared to the ones in $[(1)\text{Cp}^*\text{IrCl}]\text{Cl}$.^[15] However, the transformation of $[(1)\text{Cp}^*\text{IrCl}]\text{Cl}$ into **8** through **7** induces a distortion of the phosphinine heterocycle. Whereas the

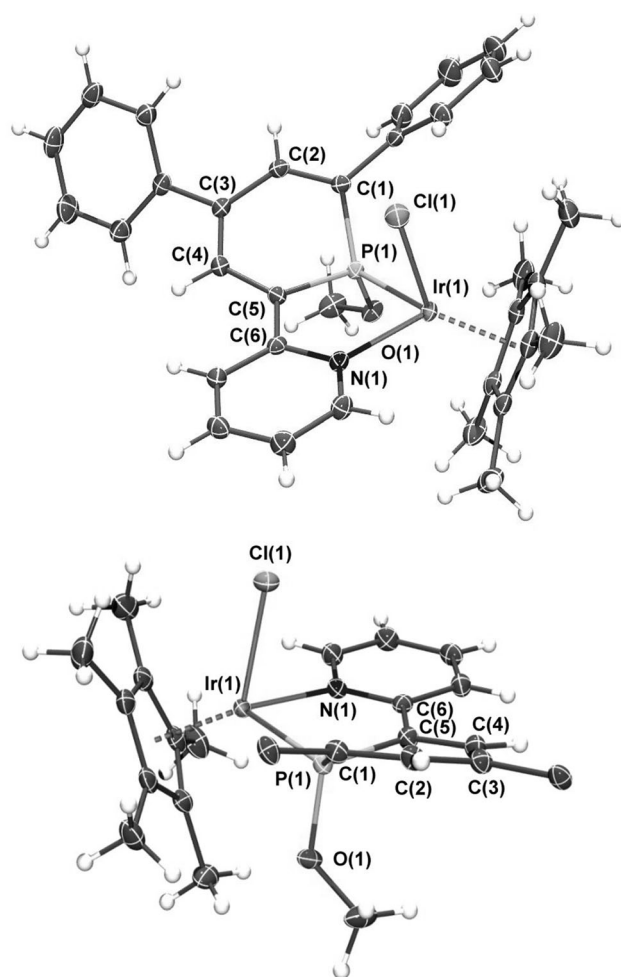
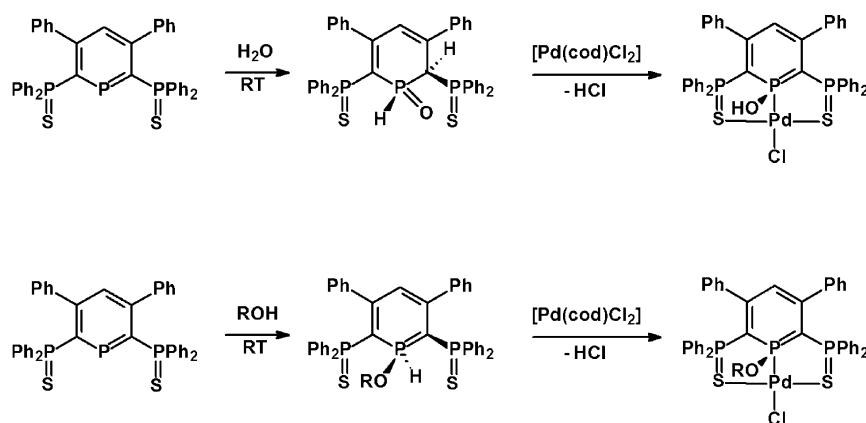


Figure 7. Molecular structure of **8** in the crystal. Displacement ellipsoids are shown at the 50% level. Bottom representation: side view along the C(5)–C(6) bond. Phenyl groups are omitted for clarity and only the *ipso*-C-atoms are shown.

phosphinine core in **6** is basically planar as mentioned above, the phosphorus atom in **8** escapes from the plane defined by the C1–C2–C3–C4–C5 atoms by as much as 0.4717(4) Å (Figure 7, bottom).

It should be mentioned here that Le Floch et al. has reported already on the synthesis of Pd-complexes containing λ^5 -SPS(OH) or λ^5 -SPS(OMe) phosphinines (Scheme 5).^[17] This route, however, is only operative because the λ^3 -SPS phosphinine already reacts with water or alcohols to form the corresponding λ^5 -phosphinines. Consequently, such reactions are generally not applicable to other phosphinines that do not react with water or alcohols, such as 2,4,6-triarylphosphinines.

In the upper reaction depicted in Scheme 5 the 1,2-dihydrophosphinine oxide reacts with $[\text{Pd}(\text{cod})\text{Cl}_2]$ upon elimination of HCl to $[\text{Pd}(\text{SPS-OH})]$, most likely through a [1,3]-H-shift from the C2 carbon atom to the P=O double bond. In the reaction using alcohols, the corresponding λ^5 -phosphinines are formed directly by a formal insertion of the phosphorus lone pair into the RO–H bond (Scheme 5, bottom).



Scheme 5. Conversion of an SPS pincer ligand into λ^5 -SPS(OH) or λ^5 -SPS(OMe) phosphinine-based Pd^{II} complexes.

These reactions are most likely the result of a significant dearomatization of the phosphorus heterocycles due to strong acceptor groups at the α position of the phosphorus atom. Nevertheless, uncoordinated 2,4,6-triphenylphosphinine derivatives, as in the case of the P,N hybrid ligand **1**, do not react with water or alcohols, making this type of conversion consequently impossible. The direct conversion of the transition-metal complexes into the new λ^5 -phosphinine(OH) and λ^5 -phosphinine(OR)-containing compounds by the reaction with water or alcohols and subsequent deprotonation, as reported here by us, is therefore an elegant and new route to such coordination compounds. We could further show, that these transformations are even possible in “one pot”, starting directly from the λ^3 -phosphinine-based [(1)Cp*MCl]Cl complexes.

DFT calculations: As evident from the X-ray crystal structure determination of compound **6** (P–OH) and **8** (P–OCH₃), the P atom deviates from the plane of the ring, although this effect is much less pronounced and hardly noticeable in **6** (Rh) in comparison to **8** (Ir). The significant

difference in the distortion of the phosphinine heterocycle in **6** and **8** suggest a different electronic situation in the phosphorus moiety of both compounds. In fact, the phosphorus-containing 6-membered ring can be described either as a $\lambda^5\sigma^4$ phosphinine consisting of an anionic $\lambda^4\sigma^3$ ligand, or, alternatively, as a $\lambda^4\sigma^4$ -phosphinine consisting of a classical tertiary $\lambda^3\sigma^3$ -phosphinite ligand (Figure 8).

To clarify this question we started to analyze the electronic properties of **6** and **8** by

means of DFT calculations starting from the corresponding X-ray crystal structures of these coordination compounds.^[18–20] All calculations were performed at the B3LYP/def2-TZVP level and the optimized structures are shown in Figure 9.

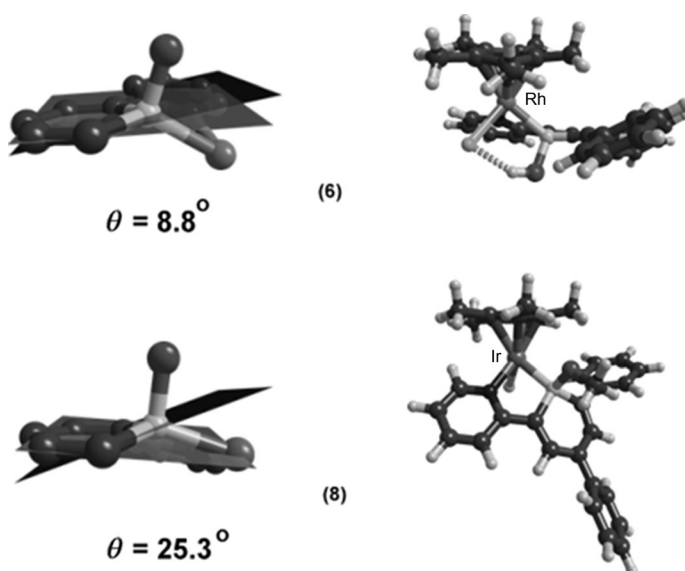


Figure 9. Optimized structures (DFT) of **6** (Rh) and **8** (Ir).

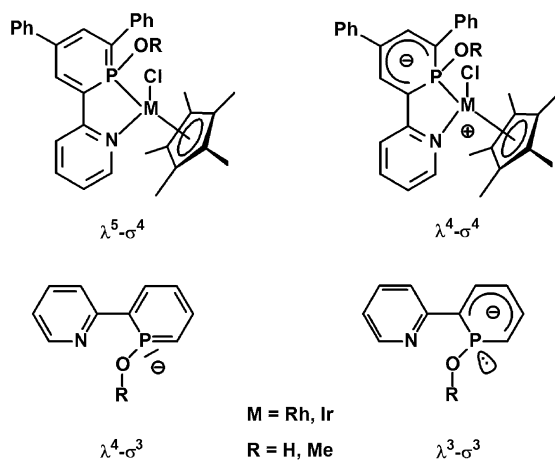


Figure 8. Resonance structures of **6** and **8** and of the corresponding ligands.

In analogy to the X-ray crystal structure determination of compound **6** (P–OH) and **8** (P–OCH₃), the P atom deviates in the optimized structures from the plane of the ring by $\theta = 8.8^\circ$ (**6**, Rh) and 25.3° (**8**, Ir), respectively. (Figure 9, left; θ corresponds to the angle between the planes of the triads of atoms of the ring).

We further analyzed the natural bond orbital (NBO) charges for both the Rh- and Ir-complex and the results are listed in Table 2.

From the results it is clear that the negative charge in both compounds is delocalized over the phosphinine ring. The total charge in the heterocycle of **6** and **8** is estimated

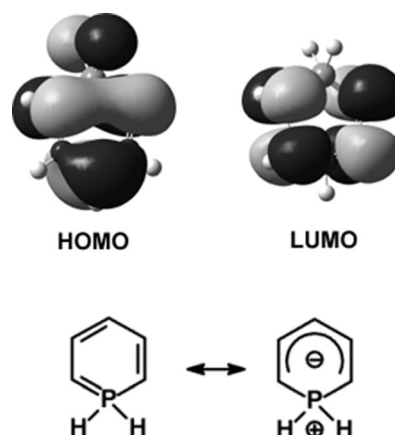
Table 2. NBO charges calculated for **6** (Rh) and **8** (Ir).

Atom/moiety	6 (Rh)	8 (Ir)
Rh/Ir	-0.236	0.085
Cl-	-0.419	-0.391
P-	+1.65	+1.545
P-benzene (approx.)	+0.67	+0.546
-OH/-OMe	-0.473	-0.498
N-	-0.360	-0.395

to be almost exactly 1 e lower than the atomic charge on P. This implies that despite the strong difference in the distortion of the phosphorus heterocycle, both compounds can best be described as a species that consists of a $\lambda^4\sigma^4$ -phosphorus heterocycle with an ylide structure. The difference in the distortion of the phosphorus heterocycle might be attributed to the presence of efficient hydrogen bonding between the P-OH group of **6** and the Cl ligand at the metal center.

We also analyzed the frontier orbitals of compound **6** and **8** and the results are depicted in Figure 10.

From Figure 10 it is obvious that the HOMO in both compounds shows a substantial delocalization over the C-P-C moiety. The metal fragment and the -OR residue at the phosphorus atom form antibonding domains within the HOMO. As a matter of fact, the shape of the HOMO strongly resembles that of the parent λ^5 -phosphinine, which is best described by an ylidic resonance structure as well

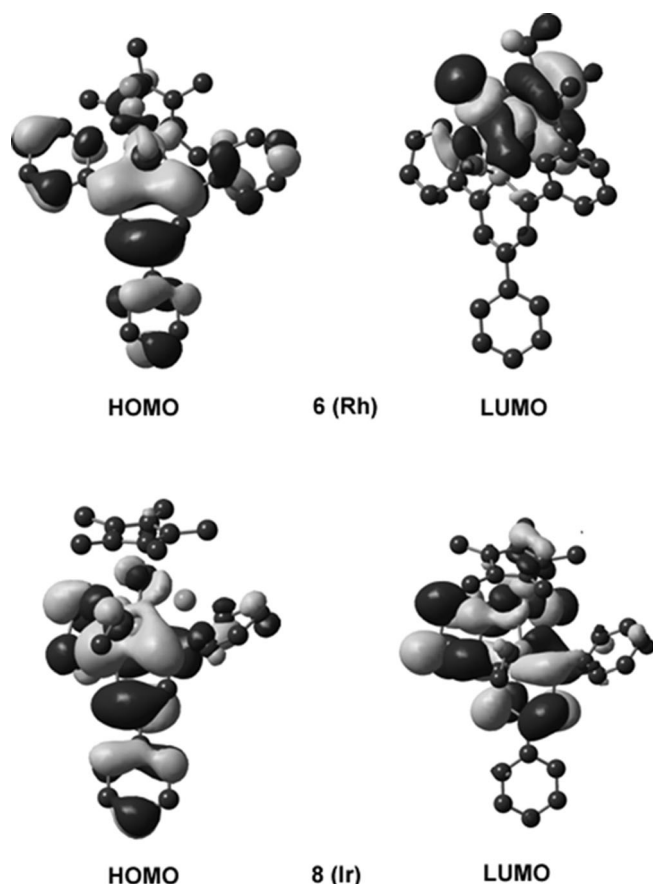
Figure 11. Frontier orbitals of the λ^5 -phosphinine $C_5H_5PH_2$.

(Figure 11).^[21] This comparison again suggests that compounds **6** and **8** are best described by the presence of a $\lambda^4\sigma^4$ -phosphorus heterocycle consisting of an ylide structure.

Nevertheless, from Figure 10 it is furthermore apparent that the LUMOs are significantly different for both compounds **6** and **8**. In both cases, there is an important contribution from the metal-centered d orbitals. Whereas in the case of compound **6** (Rh), the states due to the Cp* ligand dominate the LUMO, the LUMO of the Ir complex **8** contains substantial contribution from the bidentate ligand.

Conclusion

We have demonstrated that the cationic Rh^{III} and Ir^{III} complexes $[(1H\cdot OH)Cp^*MCl]Cl$ can be deprotonated with NEt_3 under the elimination of HCl to form zwitterionic species of the type $[(1H\cdot O)Cp^*MCl]$. By using different bases, the pK_a value of the P-OH group could be estimated ($pK_a = 5.25$). In the case of Rh^{III} , subsequent tautomerization through a [1,3]-H shift occurs and the $\lambda^5\sigma^4$ -complex $[(1\cdot OH)Cp^*RhCl]$ is formed exclusively. Starting from the corresponding $[(1H\cdot OCH_3)Cp^*IrCl]Cl$ species, in which no acid P-OH group is present, direct deprotonation of the phosphorus heterocycle was observed to form $[(1\cdot OCH_3)Cp^*IrCl]$. This transformation of λ^3 -phosphinine-based complexes into λ^5 -phosphinine(OH) and λ^5 -phosphinine(OR) complexes in the coordination environment of transition metals is a new and elegant route to such coordination compounds. It should be mentioned here, however, that the role of the pyridine moiety has not yet been clearly understood. We are currently investigating comparable reactions with Ir^{III} and Rh^{III} complexes containing cyclometalated 2-phenylphosphinines to see whether this reaction is also transposable to other phosphinine complexes. Whereas bipyridine complexes of the type $[(bpy)Cp^*RhCl]Cl$ find application in the oxidation of H_2O , it appears also attractive to further investigate the application of the here presented cationic and neutral transition-metal complexes in catalytic reactions. Research in this direction is currently being performed in our laboratories.

Figure 10. Frontier orbitals of **6** (Rh) and **8** (Ir).

Experimental Section

General: All reactions were performed under argon using Schlenk techniques or in an MBraun dry box unless stated otherwise. All glassware was dried prior to use. All common solvents and chemicals were commercially available. Coordination compounds **2** and **3** were prepared according to literature procedures.^[15] The dry solvents were prepared by using custom-made solvent purification columns filled with Al₂O₃. Elemental analyses were performed by H. Kolbe, Mikroanalytisches Laboratorium, Mülheim a. d. Ruhr (Germany). ¹H, ¹³C{¹H}, and ³¹P{¹H} NMR spectra were recorded on a Varian Mercury 400 MHz spectrometer and all chemical shifts are reported relative to residual proton resonance of the deuterated solvents.

[Cp*Ir(1H-O)Cl] (4): Compound **3** (22 mg, 0.03 mmol, 1.0 equiv) was suspended in CD₂Cl₂ (0.5 mL) and transferred to a Young NMR-Tube under argon. An excess of triethylamine (30 mg, 0.30 mmol, 10.0 equiv) was added to the mixture, which resulted in the instantaneous formation of compound **4**. The reaction mixture was filtered over celite and crystals were obtained through slow diffusion of diethylether into the reaction mixture. The yield after crystallization was 54%. ¹H NMR (CD₂Cl₂, 400 MHz): δ = 1.44 (15H, d, ³J_(H,P) = 2.3 Hz, Cp*–CH₃), 4.38 (1H, dd, ²J_(H,P) = 14.0 Hz, ³J_(H,H) = 3.2 Hz, H_a), 6.73 (1H, ddd, ³J_(H,P) = 8.4 Hz, ³J_(H,H) = 3.2 Hz, ⁵J_(H,H) = 0.8 Hz, H_b), 7.11 (1H, m, H_{arom}), 7.21 (1H, s, H_{arom}), 7.25 (1H, s, H_{arom}), 7.29 (1H, m, H_{arom}), 7.36 (4H, m, H_{arom}), 7.47 (1H, s, H_{arom}), 7.49 (1H, d, ³J_(H,H) = 1.2 Hz, H_{arom}), 7.53 (1H, s, H_{arom}), 7.55 (1H, d, ³J_(H,H) = 2.0 Hz, H_{arom}), 7.81 (1H, t, H_{arom}), 7.92 (1H, d, ³J_(H,H) = 8.0 Hz, H_{arom}), 8.66 ppm (1H, d, ³J_(H,H) = 5.6 Hz, H_{arom}); ³¹P NMR (CD₂Cl₂, 162 MHz): δ = 38.0 ppm; ¹³C NMR (CD₂Cl₂, 100.6 MHz): δ = 8.8 (–CH₃ from Cp*), 51.4 (CH), 51.0 (CH), 94.4 (d, ²J_(C,P) = 10.0 Hz, C_q from Cp*), 110.4 (C_q), 120.9 (CH), 121.0 (CH), 124.8 (CH), 126.8 (CH), 127.8 (CH), 128.4 (d, ²J_(C,P) = 8.8 Hz, CH), 128.9 (CH), 130.6 (CH), 130.6 (CH), 134.2 (d, ²J_(C,P) = 9.6 Hz, CH), 135.9 (C_q), 136.0 (C_q), 137.7 (CH), 139.8 (CH), 140.0 (CH), 140.35 (C_q), 140.39 (C_q), 140.7 (C_q), 155.6 ppm (CH).

[Cp*Rh(1-OH)Cl] (6): Compound **2** (19 mg, 0.03 mmol, 1.0 equiv) was suspended in CD₂Cl₂ (0.5 mL) and transferred to a Young NMR-Tube under argon. An excess of triethylamine (30 mg, 0.30 mmol, 10.0 equiv) was added to the mixture. Compound **5** was formed instantaneously. ¹H NMR (CD₂Cl₂, 400 MHz): δ = 1.41 (15H, d, ⁴J_(H,P) = 2.8 Hz, Cp*–CH₃), 4.65 (1H, dd, ²J_(H,P) = 12.0 Hz, ³J_(H,H) = 3.2 Hz, H_a), 6.63 (1H, ddd, ³J_(H,P) = 8.0 Hz, ³J_(H,H) = 4.0 Hz, ⁵J_(H,H) = 1.0 Hz, H_b), 7.22 (2H, t, ³J_(H,H) = 6.4 Hz, H_{arom}), 7.33 (5H, m, H_{arom}), 7.53 (5H, m, H_{arom}), 7.81 (1H, t, ³J_(H,H) = 7.8 Hz, H_{arom}), 7.91 (1H, d, ³J_(H,P) = 8.0 Hz, H_{arom}), 8.71 ppm (1H, d, ³J_(H,H) = 5.2 Hz, H_{arom}); ³¹P NMR (CD₂Cl₂, 162 MHz): δ = 80.0 ppm (d, ¹J_(Rh,P) = 133 Hz); ¹³C NMR (CD₂Cl₂, 100.6 MHz): δ = 9.2 (CH₃ from Cp*), 100.8 (C_q from Cp*), 121.1 (CH), 121.2 (CH), 124.2 (CH), 126.8 (d, ⁴J_(C,P) = 1.4 Hz, CH), 127.0 (CH), 127.1 (CH), 127.9 (CH), 128.5 (d, ⁴J_(C,P) = 2.2 Hz, CH), 128.9 (CH), 130.9 (CH), 131.0 (CH), 133.7 (CH), 133.8 (CH), 135.9 (C_q), 136.0 (C_q), 140.0 (CH), 140.1 (d, ³J_(C,P) = 3.9 Hz, C_q), 140.2 (CH), 140.8 (d, ⁴J_(C,P) = 2.9 Hz, C_q), 145.8 (C_q), 154.3 (CH), 160.3 ppm (C_q). The reaction mixture was filtered over celite and crystals of **6** were obtained through slow diffusion of diethyl ether into the reaction mixture. The yield of the isolated product after crystallization was 53%. Elemental analysis calcd (%) for C₃₂H₃₂NPOClRh–CH₂Cl₂·NEt₃ (802.06): C 58.40, H 6.1; N 3.49; found: C 58.40, H 6.10, N 3.22%.

[Cp*Ir(1H-OMe)Cl]Cl (7): Compound [(1)Cp*IrCl]Cl (22 mg, 0.03 mmol, 1.0 equiv) was suspended in CD₂Cl₂ (0.5 mL) and transferred to a Young NMR-Tube under argon. An excess of methanol (38 mg, 1.20 mmol, 40.0 equiv) was added to the mixture and compound **7** was formed instantaneously. ¹H NMR (CD₂Cl₂, 400 MHz): δ = 1.51 (15H, d, ⁴J_(H,P) = 2.8 Hz, Cp*–CH₃), 3.76 (3H, d, ³J_(H,P) = 11.2 Hz, CH₃), 4.79 (1H, dd, ²J_(H,P) = 11.2 Hz, ³J_(H,H) = 3.2 Hz, H_a), 6.95 (1H, ddd, ²J_(H,P) = 7.6 Hz, ³J_(H,H) = 3.2 Hz, ⁵J_(H,H) = 0.6 Hz, H_b), 7.38–7.54 (10H, m, H_{arom}), 7.83 (1H, s, H_{arom}), 7.88 (1H, s, H_{arom}), 8.10 (1H, t, H_{arom}), 8.22 (1H, d, ³J_(H,H) = 8.0 Hz, H_{arom}), 8.63 ppm (1H, d, ²J_(H,H) = 5.6 Hz, H_{arom}); ³¹P NMR (CD₂Cl₂, 162 MHz): δ = 77.0 ppm; ¹³C NMR (CD₂Cl₂, 100.6 MHz): 9.0 (d, ³J_(C,P) = 0.8 Hz, CH₃ from Cp*), 46.6 (CH), 50.2 (CH₃), 58.7 (d, ²J_(C,P) = 13.3 Hz, CH), 97.3 (d, ²J_(C,P) = 2.8 Hz, C_q from Cp*), 122.1 (CH), 122.2 (CH), 126.8 (d, ³J_(C,P) = 1.4 Hz, CH), 127.5 (CH), 129.1 (d, ²J_(C,P) = 3.3 Hz,

CH), 129.3 (CH), 129.5 (CH), 129.7 (d, ³J_(C,P) = 2.7 Hz, CH), 130.2 (CH), 130.3 (CH), 133.9 (C_q), 134.4 (C_q), 134.5 (d, ²J_(C,P) = 5.3 Hz, C_q), 136.8 (CH), 136.9 (CH), 138.4 (C_q), 138.9 (d, ⁴J_(C,P) = 10.1 Hz, C_q), 104.4 (CH), 141.6 (d, ³J_(C,P) = 1.6 Hz, CH), 155.9 (CH), 158.4 ppm (d, ¹J_(C,P) = 18.4 Hz, C_q). The compound was not isolated and used without further purification (see below).

[Cp*Ir(1-OMe)Cl] (8): An excess of triethylamine (30 mg, 0.30 mmol, 10.0 equiv) was added to the reaction mixture of **7** in CD₂Cl₂ in a Young NMR-Tube under argon. Compound **8** was formed instantaneously. Crystals were obtained through slow diffusion of diethyl ether into the reaction mixture. The yield after crystallization was 80%. ¹H NMR (CD₂Cl₂, 400 MHz): δ = 1.55 (15H, d, ⁴J_(H,P) = 2.4 Hz, Cp*–CH₃), 3.08 (3H, d, ³J_(H,P) = 11.6 Hz, CH₃), 6.48 (1H, m, H_b), 7.10 (1H, m, H_c), 7.23 (1H, m, H_{arom}), 7.31 (5H, m, H_{arom}), 7.40 (1H, t, H_{arom}), 7.47 (1H, d, ²J_(H,H) = 7.8 Hz, H_{arom}), 7.53 (1H, dd, ⁴J_(H,P) = 14.4 Hz, ⁴J_(H,H) = 1.2 Hz, C_{arom}), 7.58 (1H, dd, ⁴J_(H,P) = 7.2 Hz, ⁴J_(H,H) = 1.6 Hz, C_{arom}), 7.74 (2H, d, ²J_(H,H) = 8.0 Hz, C_{arom}), 7.99 ppm (1H, d, ³J_(H,H) = 6.0 Hz, C_{arom}); ³¹P NMR (CD₂Cl₂, 162 MHz): δ = 56.0 ppm; ¹³C NMR (CD₂Cl₂, 100.6 MHz): δ = 8.9 (CH₃ from Cp*), 93.8 (d, ³J_(C,P) = 3.0, C_q from Cp*), 100.4 (d, ¹J_(C,P) = 69.2 Hz, C_q), 115.0 (d, ¹J_(C,P) = 72.3 Hz, C_q), 116.5 (CH), 116.6 (CH), 117.1 (CH), 118.9 (d, ³J_(C,P) = 9.8 Hz, C_q), 124.5 (CH), 125.6 (CH), 126.1 (CH), 126.2 (CH), 128.5 (CH), 128.5 (CH), 128.7 (CH), 129.3 (d, ³J_(C,P) = 4.9 Hz, CH), 130.0 (CH), 130.1 (CH), 136.9 (CH), 139.8 (CH), 144.3 (d, ²J_(C,P) = 12.6 Hz, C_q), 144.5 (d, ⁴J_(C,P) = 1.2 Hz, C_q), 154.3 (CH), 169.1 ppm (d, ²J_(C,P) = 21.4 Hz, C_q); elemental analysis calcd (%) for C₃₃H₃₄NPOClIr–CH₂Cl₂·NEt₃ (905.40): C 53.06, H 5.68, N 3.06; found: C 54.76, H 5.63, N 3.22.

X-ray crystal-structure determinations: X-ray intensities were measured on a Bruker Kappa ApexII diffractometer with sealed tube and Triumph monochromator (λ = 0.71073 Å). The intensities were integrated by using Eval15.^[22] Absorption correction and scaling was performed with SADABS or TWINABS.^[23] The structures were solved using automated Patterson methods in the program DIRDIF-08^[24] (compound **4**) and SHELXT^[25] (compounds **6** and **8**). Least-squares refinement was performed refined with SHELXL-97^[26] against F² of all reflections. Non-hydrogen atoms were refined with anisotropic displacement parameters. Hydrogen atoms were located in difference Fourier maps (compounds **4** and **8**) or included in calculated positions (compound **6**). The O–H hydrogen atoms were refined freely with isotropic displacement parameters, whereas C–H hydrogen atoms were refined with a riding model. Geometry calculations and checking for higher symmetry was performed with the PLATON program.^[27]

Compound 4: C₃₂H₃₂ClIrNOP, *F*_w = 705.21, orange block, 0.27 × 0.13 × 0.09 mm³, orthorhombic, *Pna*2₁ (No. 33), *a* = 12.9795(3), *b* = 14.0625(3), *c* = 14.6631(3) Å, *V* = 2676.35(10) Å³, *Z* = 4, *D*_x = 1.750 g cm^{−3}, *μ* = 5.18 mm^{−1}. 43 545 Reflections were measured up to a resolution of (sin θ/λ)_{max} = 0.65 Å^{−1} at a temperature of 150(2) K. 6140 Reflections were unique (*R*_{int} = 0.030), of which 5594 were observed [*I* > 2σ(*I*)]. 340 Parameters were refined with 1 restraint. *R*₁/*wR*₂ [*I* > 2σ(*I*)] = 0.0150/0.0315. *R*₁/*wR*₂ [all refls] = 0.0189/0.0322. *S* = 1.028. Flack parameter *x* = −0.012(3).^[24] Residual electron density between −0.49 and 0.64 e Å^{−3}.

Compound 6: C₃₂H₃₂ClNOPRh·0.5(CH₂Cl₂), *F*_w = 658.38, red needle, 0.48 × 0.19 × 0.07 mm³, monoclinic, *Cc* (No. 9), *a* = 25.4883(8), *b* = 19.5808(6), *c* = 11.9853(5) Å, β = 105.322(2)°, *V* = 5769.1(3) Å³, *Z* = 8, *D*_x = 1.516 g cm^{−3}, *μ* = 0.86 mm^{−1}. The crystal appeared to be twinned with a twofold rotation about *hkl* = (1,0,0) as twin operation. The intensity integration was consequently based on two orientation matrices. 34 917 Reflections were measured up to a resolution of (sin θ/λ)_{max} = 0.65 Å^{−1} at a temperature of 150(2) K. 12 989 Reflections were unique (*R*_{int} = 0.031), of which 11 725 were observed [*I* > 2σ(*I*)]. 713 Parameters were refined with 2 restraints. *R*₁/*wR*₂ [*I* > 2σ(*I*)] = 0.0244/0.0534. *R*₁/*wR*₂ [all refls] = 0.0303/0.0550. *S* = 1.050. Flack parameter *x* = −0.013(15).^[27] Twin fraction = 0.4331(6). Residual electron density between −0.47 and 0.39 e Å^{−3}.

Compound 8: C₃₃H₃₄ClIrNOP, *F*_w = 719.23, red needle, 0.56 × 0.17 × 0.12 mm³, monoclinic, *P2*₁/*n* (No. 14), *a* = 8.6491(2), *b* = 14.3269(4), *c* = 23.3997(8) Å, β = 95.788(1)°, *V* = 2884.80(15) Å³, *Z* = 4, *D*_x = 1.656 g cm^{−3}, *μ* = 4.80 mm^{−1}. 42 821 Reflections were measured up to a resolution of (sin θ/λ)_{max} = 0.65 Å^{−1} at a temperature of 150(2) K. 6627 Reflections

were unique ($R_{\text{int}}=0.016$), of which 6106 were observed [$I > 2\sigma(I)$]. 349 Parameters were refined with no restraints. $R1/wR2$ [$I > 2\sigma(I)$]: 0.0129/0.0292. $R1/wR2$ [all refl.]: 0.0150/0.0298. $S=1.048$. Residual electron density between -0.63 and $0.42 \text{ e } \text{\AA}^{-3}$.

CCDC-904608 (4), CCDC-908560 (6), and CCDC-908561 (8) contain the supplementary crystallographic data for this paper. These data can be obtained free of charge from The Cambridge Crystallographic Data Centre via www.ccdc.cam.ac.uk/data_request/cif

Acknowledgements

This research has been funded by The Netherlands Organization for Scientific Research (NWO-Vidi and NWO-ECHO grant for C.M.). The COST-Action PhoSciNet (CM0802) is gratefully acknowledged.

- [1] See for example: a) C. Kaes, A. Katz, M. W. Hosseini, *Chem. Rev.* **2000**, *100*, 3553; b) O. Pàmies, J.-E. Bäckvall, *Chem. Eur. J.* **2001**, *7*, 5052; c) H. Yang, H. Gao, R. J. Angelici, *Organometallics* **2000**, *19*, 622; d) M. S. Lowry, S. Bernhard, *Chem. Eur. J.* **2006**, *12*, 7970; e) A. J. Esswein, D. G. Nocera, *Chem. Rev.* **2007**, *107*, 4022; f) D. A. Nicewicz, D. W. C. MacMillan, *Science* **2008**, *322*, 77; g) K. Zeitler, *Angew. Chem.* **2009**, *121*, 9969; *Angew. Chem. Int. Ed.* **2009**, *48*, 9785; h) J. D. Blakemore, N. D. Schley, D. Balcells, J. F. Hull, G. W. Olack, C. D. Incarvito, O. Eisenstein, G. W. Brudvig, R. H. Crabtree, *J. Am. Chem. Soc.* **2010**, *132*, 16017; i) A. Savini, P. Belanzoni, G. Bellachioma, C. Zuccaccia, D. Zuccaccia, A. Macchioni, *Green Chem.* **2011**, *13*, 3360; j) P. V. Pham, D. A. Nagib, D. W. C. MacMillan, *Angew. Chem.* **2011**, *123*, 6243; *Angew. Chem. Int. Ed.* **2011**, *50*, 6119; k) H. Ozawa, K. Sakai, *Chem. Commun.* **2011**, *47*, 2227.
- [2] G. Märkl, *Angew. Chem.* **1966**, *78*, 907.
- [3] A. J. Ashe III, *J. Am. Chem. Soc.* **1971**, *93*, 3293.
- [4] J.-M. Alcaraz, A. Brèque, F. Mathey, *Tetrahedron Lett.* **1982**, *23*, 1565–1568.
- [5] C. Müller, D. Wasserberg, J. J. M. Weemers, E. A. Pidko, S. Hoffmann, M. Lutz, A. L. Spek, S. C. J. Meskers, R. A. Janssen, R. A. van Santen, D. Vogt, *Chem. Eur. J.* **2007**, *13*, 4548–4559.
- [6] A. Campos-Carrasco, E. A. Pidko, A. M. Masdeu-Bultó, M. Lutz, A. L. Spek, D. Vogt, C. Müller, *New J. Chem.* **2010**, *34*, 1547–1550.
- [7] A. Campos-Carrasco, L. E. E. Broeckx, J. J. M. Weemers, E. A. Pidko, M. Lutz, A. M. Masdeu-Bultó, D. Vogt, C. Müller, *Chem. Eur. J.* **2011**, *17*, 2510–2517.
- [8] C. Müller, D. Vogt in *Catalysis and Material Science Applications*, Vol. 36, Chapter 6 (Eds.: M. Peruzzini, L. Gonsalvi), Springer, Heidelberg, **2011**.
- [9] C. Müller, D. Vogt, *Dalton Trans.* **2007**, 5505.
- [10] P. Le Floch, *Coord. Chem. Rev.* **2006**, *250*, 627.
- [11] N. Mézailles, F. Mathey, P. Le Floch, *Prog. Inorg. Chem.* **2001**, *49–50*, 455.
- [12] P. Le Floch, F. Mathey, *Coord. Chem. Rev.* **1998**, *178–180*, 771.
- [13] C. Müller, L. E. E. Broeckx, I. de Krom, J. J. M. Weemers, *Eur. J. Inorg. Chem.* **2013**, 187.
- [14] P. Le Floch, S. Mansuy, L. Ricard, F. Mathey, *Organometallics* **1996**, *15*, 3267.
- [15] B. Schmid, L. M. Venanzi, A. Albinati, F. Mathey, *Inorg. Chem.* **1991**, *30*, 4693.
- [16] I. de Krom, L. E. E. Broeckx, M. Lutz, C. Müller, *Chem. Eur. J.* **2013**, *19*, 3676–3684.
- [17] M. Doux, N. Mézailles, L. Ricard, P. Le Floch, *Eur. J. Inorg. Chem.* **2003**, 3878.
- [18] DFT calculations were carried out by using the Gaussian 09 program at the B3LYP/def2-TZVP level of theory (see ref. [19]). The nature of the stationary points was tested by analyzing the analytically calculated harmonic normal modes. Optimized structures did not show imaginary frequencies.
- [19] Gaussian 09, Revision A.01, M. J. Frisch, G. W. Trucks, H. B. Schlegel, G. E. Scuseria, M. A. Robb, J. R. Cheeseman, G. Scalmani, V. Barone, B. Mennucci, G. A. Petersson, H. Nakatsuji, M. Caricato, X. Li, H. P. Hratchian, A. F. Izmaylov, J. Bloino, G. Zheng, J. L. Sonnenberg, M. Hada, M. Ehara, K. Toyota, R. Fukuda, J. Hasegawa, M. Ishida, T. Nakajima, Y. Honda, O. Kitao, H. Nakai, T. Vreven, J. A. Montgomery, Jr., J. E. Peralta, F. Ogliaro, M. Bearpark, J. J. Heyd, E. Brothers, K. N. Kudin, V. N. Staroverov, R. Kobayashi, J. Normand, K. Raghavachari, A. Rendell, J. C. Burant, S. S. Iyengar, J. Tomasi, M. Cossi, N. Rega, J. M. Millam, M. Klene, J. E. Knox, J. B. Cross, V. Bakken, C. Adamo, J. Jaramillo, R. Gomperts, R. E. Stratmann, O. Yazyev, A. J. Austin, R. Cammi, C. Pomelli, J. W. Ochterski, R. L. Martin, K. Morokuma, V. G. Zakrzewski, G. A. Voth, P. Salvador, J. J. Dannenberg, S. Dapprich, A. D. Daniels, Ö. Farkas, J. B. Foresman, J. V. Ortiz, J. Cioslowski, D. J. Fox, Gaussian, Inc., Wallingford CT, **2009**.
- [20] a) F. Weigend, R. Ahlrichs, *Phys. Chem. Chem. Phys.* **2005**, *7*, 3297; b) D. Andrae, U. Haeussermann, M. Dolg, H. Stoll, H. Preuss, *Theor. Chim. Acta* **1990**, *77*, 123.
- [21] Z.-X. Wang, P. von Ragué Schleyer, *Helv. Chim. Acta* **2001**, *84*, 1578.
- [22] A. M. M. Schreurs, X. Xian, L. M. J. Kroon-Batenburg, *J. Appl. Crystallogr.* **2010**, *43*, 70–82.
- [23] G. M. Sheldrick, *SADABS and TWINABS, Area-Detector Absorption Correction*, v 2.10, Universität Göttingen, Germany, **1999**.
- [24] P. T. Beurskens, G. Beurskens, R. de Gelder, S. Garcia-Granda, R. O. Gould, and J. M. M. Smits, *The DIRDIF2008 program system*, Crystallography Laboratory, University of Nijmegen, The Netherlands, **2008**.
- [25] G. M. Sheldrick, *SHELXT*, Universität Göttingen, Germany, **2012**.
- [26] G. M. Sheldrick, *Acta Crystallogr.* **2008**, *A64*, 112–122.
- [27] A. L. Spek, *Acta Crystallogr.* **2009**, *D65*, 148–155.
- [28] H. D. Flack, *Acta Crystallogr.* **1983**, *A39*, 876–881.

Received: January 28, 2013
Published online: April 4, 2013